Supporting Information

Hetero atom (boron, nitrogen, and fluorine) quantum dot doped polyaniline-photoactive film preparation and characterization for organic solar cell applications

Esakkimuthu Shanmugasundaram[a], Vigneshkumar Ganesan[a], Vimalasruthi Narayanan[a], Kannan Vellaisamy[a] Rajaram Rajamohan[b*], Yong Rok Lee[b*], Selvam Kaliyamoorthy[c], Stalin Thambusamy[a]**

[a] Department of Industrial Chemistry, Alagappa University, Karaikudi - 630 003, India.

[b] Organic Materials Synthesis Lab, School of Chemical Engineering, Yeungnam University, Gyeongsan 38541, Republic of Korea.

[c] The Noyori Laboratory, Graduate School of Science and Research Center for Materials Science,

Nagoya University, Furo-Cho, Chikusa-ku, Nagoya 464-8602, Japan.

Corresponding author: *rajmohanau@yu.ac.kr, **yrlee@yu.ac.kr, ***stalin.t@alagappauniversity.ac.in

1. Characterization Techniques

CQD and CQD-doped PANI photoactive films' absorbance and fluorescence behaviour are studied by JASCO NIS 670 (liquid) UV-VISIBLE SPECTROPHOTOMETER and JASCO FP-8200 Spectro fluorometer in the range of 200 to 800 nm. The 1 mL of concentrated CQD solution was diluted in 100 mL of deionized water. Then, 2 mL of diluted CQDs are taken in a quartz cuvette (3.5 mL-volume, width-10mm, Dimension-45*12.5*12.5 mm) for analysis. The PANI photoactive films' absorbance was studied by JASCO NIS 670 (SOLID) UV-Visible spectrophotometer and JASCO FP-8200 Spectrofluorometer. The functional group was identified by JASCO 4600 Fourier transform infrared spectrometer (FT-IR) in Attenuated Total Reflectance (ATR) Accessories mode (Resolution: 0.7 cm^{-1}) in the range of 400-4000 cm^{-1}. The electrochemical polymerization and electrochemical studies were done by metrohm electrochemical analyzer MULTIAUTOLAB-M204 (NOVA software) with three electrodes set up FTO act as a working electrode (1 × 1 surface area), Ag/AgCl as a reference electrode and platinum wire (1 × 1 surface area), as a counter electrode. The electrochemical characterization such as cyclic voltammetry and electrochemical impedance spectroscopy was done by 1M H_2SO_4 electrolyte. The functional group was studied by x-ray diffractometer (XRD - X' Pert Pro – PANalytic) equipped with a Cu Kα source (1.54 Å - wavelength, Scan step size-0.0500^{o,} scan step time-10.7950s). Raman spectroscopy was done by XploRA™ PLUS Raman Spectrometer - Confocal Raman Microscope (wavelength range - 200-1050 nm, wave number -100 cm^{-1} to 4000 cm^{-1}, power-reflection (LED eqv 100 W)/ transmission (Halogen 30 W), spot size-20X (NA=0.4

WD=1.3mm), 100(NA=0.9 WD=0.21mm, scan step size - 10nm, repeatability-1μm; resolution - 100 nm, FLAT fluorescence subtraction). LabSpec6 spectral software was used to analyse the Raman data. The surface morphology was studied by Field emission scanning electron microscopy (SU08010), sample preparation – the conductive sample plates were directed and placed in a sample stage and calibrated, accelerating voltage - 0.1 ~ 30kV (with deceleration) current- 300 μA) Resolution-1.0 nm@15kV /1.3nm @1 kV, photo magnification -×20 -×800,000 (Photo magnification) ×60 -×2,000,000 (Display magnification). The I-V response of the photoactive films was tested by biologic instrument SP-200 equipped with solar stimulator (AM 1.5G - 85 mW/cm^2). The electropolymerized polymer electrodes (1×1 surface area) are an active layer. The carbon was coated on the active layer (screen printing method), the thickness is one micron which is used as a back electrode.

The Density functional theory (DFT) of CQDs was carried out by Gaussian 16. The structure of CQD and heteroatom-doped CQDs structure are constructed like a graphene structure and optimized[1,2]. The study employs the B3LYP exchange–correlation function with 6-31+G (d,p) basis set[3]. The molecule modeling method was given the minimum energy and optimized structure of CQDs and the highest occupied and lowest unoccupied molecular orbitals (HOMO&LUMO). The resultant HOMO-LUMO Hartree values are converted into the eV and calculated the band gap value with the help of the below equation

$$\text{band gap energy} = \text{HOMO-LUMO (eV)} \quad (1)$$

2. Proposed Mechanism

2.1. Upconversion CQD mechanism

Ascorbic acid-derived CQD has upconversion properties that can improve the photophysical properties of the dopant materials. The ascorbic acid band gap is 5 eV. When it involves a hydrothermal process, it converts to CQD with a low band gap. The CQD contains different sizes of quantum with various band gap structures based on the size. That size difference gives the upconversion behaviour to the CQD. Upconversion is an anti-stoke transition. It contains two ground state multiplicity σ and π orbitals. Hoffmann proposed the upconversion material energy difference (E) should be below 1.5 eV[4]**.** In our previous work, the CQD energy difference was calculated based on the below formula (1)

$$Em = 1.00Ex + \delta E \ (R^2 = 0.96674) \qquad (1)$$

(Ex-Excitation light and Em-Emission light)

and reported the range is δE = 0.99 eV. Normally, the photons excite the electron from the σ orbital and reach the electron in the highest occupied molecular orbital (HOMO) and return to the lowest unoccupied molecular orbital (LUMO) that process can emit light is called fluorescence. The CQD upconversion mechanism is different from the normal fluorescence mechanism. Instead of σ orbital, the lower energy photon (higher wavelength) excites the electron in the π orbital and returns to the σ orbital, and emits a higher energy photon (lower wavelength). The higher energy transfer to the higher band gap material for electron excitation because this process reduces wavelength vs band gap mismatch problems.

2.2. Förster resonance energy transfer (FRET) mechanism between the polyaniline – Upconversion CQD

The upconversion CQD easily excites the lower energy photons and emits the higher energy photons. Mostly, organic polymers are used as donor molecules in organic solar cell (OSC)

applications. However, the PANI cannot be used for OSC because the band gap range is < 3.5 eV, it only absorbs visible regions (higher energy). It is a well-known fact that if the large band gap polymers are doped with photosensitizers, it involves Förster resonance energy transfer (FRET) process and converts higher and lower light energy into electrical energy[5]. When the CQD is doped with the PANI, the CQD can convert the higher energy photons from the solar source and convert them to the lower energy photons that energy suitable for PANI excitation. So, the PANI and CQD involve the FRET process and the PANI excites more electrons that can improve the efficiency of the solar cell. In this work, the heteroatom doped with the CQD enhances the photophysical property of the CQD and improves the efficiency of the PANI light-harvesting property. The schematic illustration upconversion fluorescence emission process of CQD and the FRET mechanism between PANI and CQD.

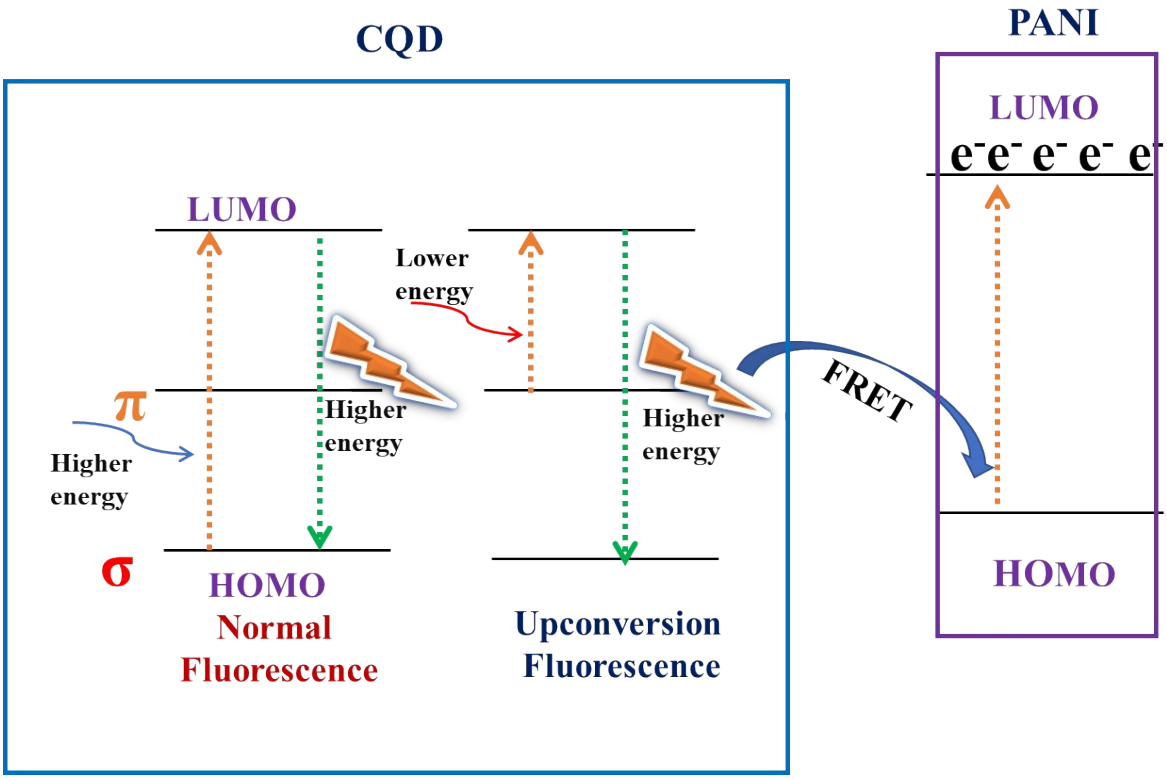

Scheme S1. Schematic illustration of upconversion fluorescence emission process of CQD and the FRET mechanism between PANI and CQD.

3. Mass production and quantum yield calculation:

The mass production[6] and quantum yield (QY)[7-9] of the CQDs are calculated and reported in Table S1. The CQDs QY was calculated by the comparison of the wavelength-integrated intensity of the CQDs samples with a standard. Quinine sulfate was used as a reference QY standard (QY=0.54)[10]. William's comparative method was used to calculate the QY value (ϕF) of the CQD samples. The equation (2) of (ϕF) calculation is

$$QYx = Fx \times As \times QYs / Fs \times Ax \qquad (2)$$

where, QYx - Quantum yield of CQDs, Fx- Integrated fluorescence emission of CQD, Fs- Integrated fluorescence emission of standard Quinine sulfate, As - Quinine sulfate absorbance at the excitation wavelength, QYs- Quantum yield of Quinine sulfate.

Compared to others, N-CQD has higher mass production and quantum yield. The nitrogen heteroatom doping in the CQD by bonding to the carbon atom. The nitrogen has a negative charge whereas, the CQD carbon has a positive charge, indicating the charge transfer between the nitrogen to carbon atoms. The charge transfer caused by the nitrogen heteroatom is a reason for the high quantum yield of N-CQD. The F-CQD also creates charge transfer behavior but the quantum yield is lower than N-CQD due to the higher electronegativity of fluorine and carbon. The difference can decrease the orbital overlap property so that the charge transfer behavior is minimized.

Table S1. Mass production and Quantum yield Calculation.

Raw material	Product	Reaction method	Reaction times	Production yields	Conversion yields	Quantum yields
Ascorbic acid	CQD	Hydrothermal	6h	0.57 g	28%	2.40%
Ascorbic Acid + Boric acid	B-CQD	Hydrothermal	6h	1.26 g	42%	1.55%
Ascorbic Acid + Urea	N-CQD	Hydrothermal	6h	1.55 g	52%	8.94%
Ascorbic Acid + Sodium fluoride	F-CQD	Hydrothermal	6h	1.34 g	45%	3.16%

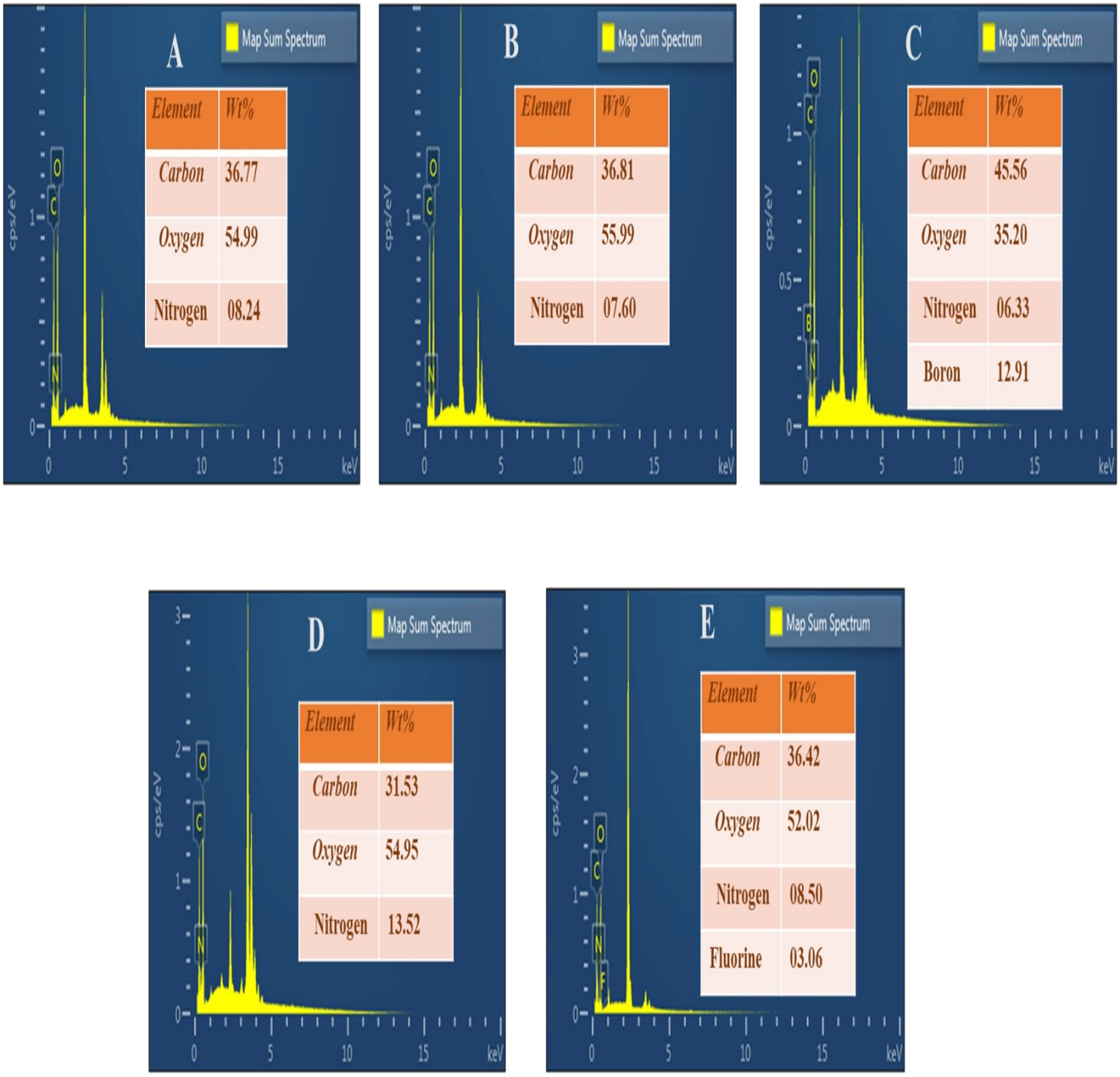

Figure S1. EDAX elemental analysis study of PANI **(A)**, PANI-CQD **(B)**, PANI-B-CQD **(C)**, PANI-N-CQD **(D)**, PANI-F-CQD **(E)**.

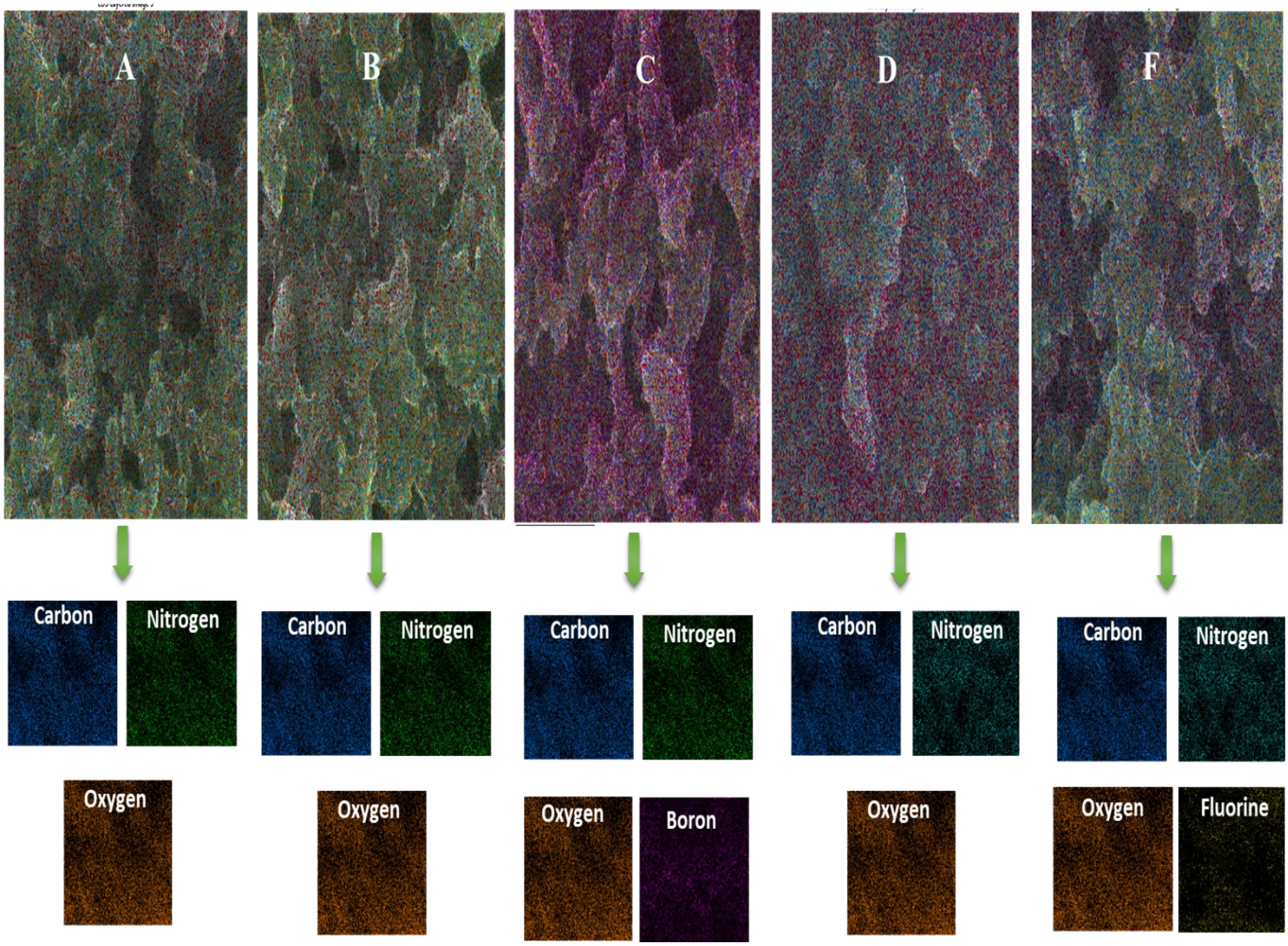

Figure S2. EDAX mapping study of PANI **(A)**, PANI-CQD **(B)**, PANI-B-CQD **(C)**, PANI-N-CQD **(D)**, and PANI-F-CQD **(E)**.

References

1. A. R. Sadrolhosseini, S. A. Rashid, N. Jamaluddin and A. M. Isloor, Experimental and molecular modeling of interaction of carbon quantum dots with glucose, *Applied Physics A.,* 2019, **125**, 529.

2. P. Zhang, Q. Hu, X. Yang, X. Hou, J. Mi, L. Liu and M. D. Dong, Size effect of oxygen reduction reaction on nitrogen-doped graphene quantum dots, *RSC Adv*., 2018, **8**, 531.

3. L.H. Nguven, A computational study of the electronic properties od hetero circulenes: oxiflowers and sulflowes, *ACS Omega*, 2021, **6**, 44, 30085-30092.

4. J. Shen, Y. Zhu, C. Chen, X. Yang and C. Li, Facile preparation and upconversion luminescence of graphene quantum dots*, Chem. Commun*., 2011, **47**, 2580-2582.

5. A. Bruno, C. Borriello, S. A. Haque, C. Minarini and T. D. Luccio, Ternary hybrid systems of P3HT–CdSe–WS_2 nanotubes for photovoltaic applications, *Phys. Chem. Chem. Phys.,* 2014, **16**, 17998.

6. J. Ma, L. Zhang, X. Chen, R. Su, Q. Shi, S.Zhao, Q. Xu and C. Xu ,Mass production of highly fluorescent full color carbon dots from the petroleum coke, *Chin. Chem. Lett.,* 2021, **32,** 1532-1536.

7. Y. Liu, J. Wei, X. Yan, M. Zhao, C. Guo and Q. Xu, Barium charge transferred doped carbon dots with ultra-high quantum yield photoluminescence of 99.6% and applications, *Chin. Chem. Lett., 2021,* **32**, 861-865.

8. B. Tang, Y. Lu, J. Zhou, T. Chouhan, H. Wang, P. Golani, M. Xu, Q. Xu, C. Guan and Z. Liu, Machine learning-guided synthesis of advanced inorganic materials, *Mater. Today.,*2020, **41**, 72-80.

9. S. Li, H. Zheng, L. Ding, X. Xiao, Y. Niu, Y. Tang, Z. Liu, W. Zhang, Y. Zhou and Q. Xu, Machine learning guided full-color V4C3 MXene quantum dots for building WLEDs, *J. Mater. Chem. C*, 2022, **10**, 14282-14287.

10. M. Maruthupandi, D. Thiruppathi, and N. Vasimalai, One minute synthesis of green fluorescent copper nanocluster: The preparation of smartphone aided paper-based kit for on-site monitoring of nanomolar level mercury and sulfide ions in environmental samples, *J. Hazard. Mater.,*2020, **392,** 122294.